GRAPH-BASED JOINT DENOISING AND SUPER-RESOLUTION OF GENERALIZED PIECEWISE SMOOTH IMAGES

Wei Hu [*], *Gene Cheung* [#], *Xin Li* [$], *Oscar C. Au* [*]

[*] Hong Kong University of Science & Technology, Hong Kong [#] National Institute of Informatics, Japan
[$] West Virginia University, USA

ABSTRACT

Images are often decoded with noise at receiver due to capturing errors and/or signal quantization during compression. Further, it is often necessary to display a decoded image at a higher resolution than the captured one, given available high-resolution (HR) display or a need to zoom-in for detailed examination. In this paper, we address the problems of image denoising and super-resolution (SR) jointly in one unified graph-based framework, focusing on a special class of signals called generalized piecewise smooth (GPWS) images. GPWS images are composed mostly of smooth regions connected by transition regions, and represent an important subclass of images, including cartoon, sub-regions of video frames with captions, graphics images in video games, etc. Like our previous work on piecewise smooth (PWS) images, GPWS images also imply simple-enough graph representations in the pixel domain, so that suitable graph-based filtering techniques can be readily applied. Specifically, leveraging on previous work on graph spectral analysis, for a given pixel block in low-resolution (LR) we first use the second eigenvector of a computed graph Laplacian matrix to identify a hard boundary, and then use the third eigenvector to identify two piecewise smooth regions and a transition region that separates them. The LR hard boundary is then super-resolved into HR via a procedure based on local self-similarity, while graph weights of the LR transition region is mapped to those of the HR transition region via polynomial fitting. Using the computed HR boundary and weights in the transition region, we construct a suitable HR graph corresponding to the LR counterpart, and perform joint denoising / SR using a graph smoothness prior. Experimental results show that our proposed algorithm outperforms two representative separable denoising / SR schemes in both subjective and objective quality.

***Index Terms*—** Graph signal processing, image denoising, super-resolution, piecewise-smooth signals

1. INTRODUCTION

Despite continuing progress in camera and network technologies, images are still often decoded at a user corrupted with noise, due to either errors in the capturing process, or lossy compression stemming from storage / bandwidth limitations. Further, decoded images are often expected to be super-resolved into higher resolution, either for now popular ultra high-definition displays (*e.g.*, 4k TV), or for zoom-in operations to examine details of the image. While the problems of image denoising and super-resolution (SR) can be handled independently in separate stages, this divide-and-conquer approach is in general sub-optimal. The reason is that denoising algorithms are usually not capable of removing the entire noise component in a corrupted low-resolution (LR) image (without destroying texture details in the original image), and so a subsequent SR process can mistakenly amplify the leftover noise, resulting in poor visual quality in the reconstructed high-resolution (HR) image.

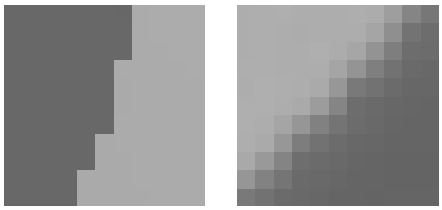

(a) PWS image (b) GPWS image

Fig. 1. Examples of piecewise smooth (PWS) and generalized piecewise smooth (GPWS) images.

In this paper, we propose to address the problems of image denoising and SR jointly for a special class of images with *generalized piecewise smooth* (GPWS) characteristics. In our previous work [1, 2], we have studied the compression and denoising of piecewise smooth (PWS) images such as depth maps in a graph formulation, where a PWS image is composed of spatially smooth regions separated by sharp boundaries. GPWS images are similar to PWS images but with a non-sharp transition region between two smooth regions. GPWS images can be found commonly in mass media, *e.g.*, cartoon images, logo images, sub-regions of video frames with overlaid language captions, visual saliency maps [3], graphics images in video games[1], etc. See Fig. 1 for examples of PWS and GPWS image patches.

Leveraging on recent advances in *graph signal processing* (GSP) [4], we propose to jointly solve the GPWS image denoising and SR problems in one unified graph-theoretic framework. The key observation is that a GPWS image implies a simple-enough graph representation in the pixel domain—where an edge connecting two vertices contains a weight that reflects the intensity difference between two adjacent pixels—so that graph-based filtering techniques [5] can be readily applied. The graph representation of a GPWS pixel patch can be derived naturally via segmentation into smooth and transition regions via spectral clustering [6]. Specifically, for a given LR pixel patch, we first use the second eigenvector of a computed graph Laplacian matrix to identify a *hard boundary* (which defines the shape of the transition region), and then use the third eigenvector to identify *borders* between smooth and transition

This work is supported in part by Hong Kong Research Grant Council GRF, Innovation and Technology Fund, and the State Key Laboratory on Advanced Displays and Optoelectronics Technologies (Project No: ITC-PSKL12EG02).

[1] Video games played by experts are broadcasted live as compressed video to a mass audience in South Korea. One usage of our proposed algorithm is to enhance image quality of decoded game video in real-time.

regions. The LR hard boundary is then super-resolved into HR via a procedure based on local self-similarity [7], while graph weights of the LR transition region is mapped to those of the HR transition region via polynomial fitting. Using the computed HR boundary and weights in the transition region, we construct a suitable HR graph corresponding to the LR counterpart, and perform joint denoising / SR using a graph smoothness prior. Experimental results show that our proposed algorithm outperforms two representative separable denoising / SR schemes in both subjective and objective quality.

The outline of the paper is as follows. We first discuss related work in Section 2. We then review GSP tools in Section 3 and overview our proposed joint denoising / SR algorithm in Section 4. Section 5 describes in detail our proposed problem formulation and algorithm. Experimentation and conclusion are presented in Section 6 and 7, respectively.

2. RELATED WORK

There are extensive research on image denoising and SR, but the two problems are typically studied independently. Instead, [8, 9] performed denoising and color demosaicking (a special case of SR) under a unified framework. [10] proposed to jointly train two dictionaries for the LR and HR image patches and enforce similarity of sparse representations between them. The computational complexity of dictionary training, however, is a hurdle for real-time implementation. [11] modeled denoising and SR under the same linear minimum mean square-error estimation (LMMSE) framework to estimate both the noiseless and missing samples from the noisy and LR image. Unlike [11], our joint denoising / SR algorithm exploits the GPWS characteristics and thus is more computation-efficient.

Leveraging on spectral graph theory [12], GSP is the study of signals on structured data kernels described by graphs [4, 13]. GSP can also be applied to signals on regular kernels, such as an image on a 2D grid, where the signal structure is embedded into the definition of the graph before GSP tools are applied to the signal. In our previous work [1, 2], we studied the compression and denoising of PWS images in the graph domain. Our current work on GPWS images can be interpreted as an extension of our previous work, where a GPWS signal is a generalization of a PWS signal.

3. SPECTRAL GRAPH THEORY

Spectral graph theory [12] studies the properties of a graph in terms of the characteristic polynomial, eigenvalues and eigenvectors of matrices associated with the graph, such as adjacency or Laplacian matrices. A weighted graph $\mathcal{G} = \{\mathcal{V}, \mathcal{E}, \mathbf{W}\}$ consists of a finite set of vertices $\mathcal{V}$ with cardinality $|\mathcal{V}| = N$, a set of edges $\mathcal{E}$ connecting vertices, and a weighted adjacency matrix $\mathbf{W}$. $\mathbf{W}$ is a real $N \times N$ matrix where $W_{i,j}$ is the weight assigned to the edge connecting vertices i and j. We consider here only undirected graphs, which correspond to symmetric weighted adjacency matrices, *i.e.*, $W_{i,j} = W_{j,i}$. We also assume that the weights are non-negative, *i.e.*, $W_{i,j} \geq 0$.

The unnormalized combinatorial graph Laplacian is defined as $\mathcal{L} := \mathbf{D} - \mathbf{W}$, where $\mathbf{D}$ is the *degree matrix*—a diagonal matrix where the ith diagonal element is the sum of all elements in the ith row of $\mathbf{W}$, *i.e.*, $D_{i,i} = \sum_{j=1}^{N} W_{i,j}$.

Since the Laplacian matrix is a real symmetric matrix, it admits a set of real eigenvalues $\{\lambda_l\}_{l=1,...,N}$ with a complete set of orthonormal eigenvectors $\{\psi_l\}_{l=1,...,N}$, *i.e.*, $\mathcal{L}\psi_l = \lambda_l \psi_l$, for $l = 1, ..., N$. Note that zero appears as an eigenvalue with multiplicity equal to the number of connected components in the graph [12].

3.1. Spectral Clustering

Clustering, identification of sub-groups of similar data, has been widely used for exploratory data analysis. In particular, spectral clustering [6] has emerged as one of the most popular modern clustering techniques. In general, spectral clustering deploys the first k eigenvectors $\{\psi_l\}_{l=1,...,k}$ of the Laplacian matrix for the construction of k clusters in the data. There exist a family of spectral clustering algorithms, such as the well-known Normalized Cuts [14].

In this work, we use the second eigenvector ψ_2 to identify the hard boundary in a pixel patch (shape of transition region) and the third eigenvector ψ_3 to identify the borders between smooth / transition regions. An example is illustrated in Fig. 2.

(a) image patch (b) ψ_2 (c) ψ_3

Fig. 2. An example of the *hard boundary* and *borders* of smooth and transition regions in a GPWS signal: (a) GPWS image patch; (b) the corresponding second eigenvector of the graph Laplacian, using which the hard boundary can be identified; (c) the corresponding third eigenvector, using which the borders of the smooth / transition regions can be identified.

3.2. The Smoothness Interpretation of Graph Signals

The graph Laplacian can be used to describe the total variation of the signal with respect to the graph, *i.e.*, for any signal $\mathbf{x} \in \mathbb{R}^N$ residing on the vertices of the graph represented by $\mathcal{L}$, we can write [6]

$$\mathbf{x}^T \mathcal{L} \mathbf{x} = \frac{1}{2} \sum_{i=1}^{N} \sum_{j=1}^{N} W_{i,j} (x_i - x_j)^2 \quad (1)$$

$\mathbf{x}^T \mathcal{L} \mathbf{x}$ is small when $\mathbf{x}$ has similar values at each pair of vertices i and j connected by an edge, or when the weight $W_{i,j}$ is small for an edge connecting i and j with dissimilar values. Hence, *a signal is smooth with respect to a graph if the graph weights well capture the underlying structure of the signal*.

4. SYSTEM OVERVIEW

Given GPWS images are composed of mostly smooth regions connected by transition regions (see Fig. 1 for an example), our joint denoising / SR system is based on the observation that the appropriate graph structure for a GPWS image patch is relatively simple and can be derived easily from observed LR image pixels. After the appropriate graph is computed for the target HR patch (one corresponding to the observed LR patch), simple graph filtering operations can be performed for joint denoising / SR to reconstruct the HR signal.

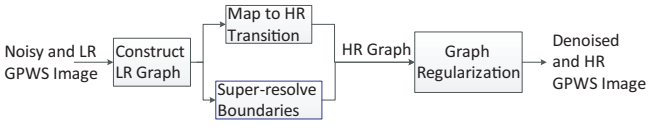

Fig. 3. Framework of our proposed joint denoising / SR of GPWS images.

Specifically, given an input noisy and LR GPWS image, we divide it into non-overlapping patches of size $\sqrt{N} \times \sqrt{N}$ (*e.g.*, $\sqrt{N} =$

8) and super-resolve each patch to a $M\sqrt{N} \times M\sqrt{N}$ HR patch for an up-sampling factor M. As shown in Fig. 3, for each LR patch we perform the following three steps to reconstruct the corresponding HR patch:

1. Construct a graph for the LR patch, and identify via spectral clustering the *hard boundary* and the *borders* between smooth and transition regions to compute appropriate graph weights. (See Fig. 2 for examples of hard boundary and smooth / transition region borders.) If the LR patch is detected by spectral clustering to be entirely smooth, then we construct a graph with all weights 1.
2. Given the constructed LR graph, construct a HR graph for the HR latent signal, where we construct the HR hard boundary from the LR one via local self-examples as done in [7], and derive the HR transition region from the LR counterpart. For entirely smooth patches, we simply construct a HR graph where all weights are 1 accordingly.
3. Formulate the joint denoising / SR as an optimization problem, with a smoothness prior for the HR signal using the HR graph constructed in the previous step.

5. PROBLEM FORMULATION

The key to our proposed joint denoising / SR of GPWS images is the derivation of an appropriate graph representation for the latent HR signal from the observed LR counterpart. A subsequent optimization regularized by a smoothness prior with respect to the constructed HR graph can then be readily performed to acquire the reconstructed signal. Hence, we first elaborate on the two-step procedure of the derivation of the HR graph for each image patch, including the construction of the LR graph in Subsection 5.1 and the construction of the HR graph from the LR graph in Subsection 5.2. Then we arrive at the problem formulation using the derived HR graph.

5.1. Construction of the LR Graph

For the construction of the LR graph, we first identify the hard boundary and borders between smooth / transition regions via spectral clustering. Then we compute edge weights in the transition regions using an averaging kernel along the orientation of the identified hard boundary, resulting in robust weight estimation. Edge weights within the borders of smooth regions are simply assigned the value 1.

5.1.1. Identification of LR Hard Boundary & Borders

In order to employ spectral clustering for the identification of the hard boundary and borders between smooth / transition regions, we first construct a four-connectivity graph for each observed LR image patch. The edge weight $\tilde{W}_{i,j}$ between adjacent pixels i and j is estimated by their intensity similarity:

$$\tilde{W}_{i,j} = \exp\left\{\frac{-|y_i - y_j|^2}{\sigma_w^2}\right\}, \tag{2}$$

where y_i and y_j are the intensities of pixel i and j. σ_w controls the sensitivity of the similarity measure to the noise and the range of the intensity difference.

Second, we compute the graph Laplacian matrix $\mathcal{L}_l$ from the edge weights, and identify the hard boundary and borders between smooth / transition regions using the second and third eigenvectors of $\mathcal{L}_l$ respectively, as described in Sec. 3. The segmentation into smooth and transition regions is critical for the subsequent denoising and SR, because it enables the preservation of image sharpness during joint denoising / SR, as will be discussed later.

5.1.2. Robust Weight Estimation in the LR Transition Region

Having identified the LR hard boundary and borders between smooth / transition regions, we compute weights within the borders of the LR transition region by an averaging kernel along the orientation of the hard boundary for robust weight estimation.

Inspired by the concept of *Steering Kernel* in [15], the averaging kernel averages pixels along the orientation of the detected hard boundary to effect denoising strongly along the hard boundary. Weights in the transition region are then robustly computed as in (2). Averaging over multiple pixel values along the orientation of the hard boundary results in robust weight estimation, while preserving details perpendicular to the hard boundary.

Note that while [15] uses singular value decomposition for the estimation of the dominant orientation for denoising, which is computational expensive, we use the orientation of the identified hard boundary directly, which is simple yet robust.

5.2. Construction of the HR Graph from the LR Graph

Given the constructed LR graph, we now derive the corresponding HR graph. We first super-resolve the hard boundary, which dictates the shape of the transition region. Then we derive the HR borders between the smooth / transition regions and estimate weights in the HR transition region. Weights within the HR borders of smooth regions are assigned 1.

5.2.1. Estimation of the HR Hard Boundary

Given the identified LR hard boundary, we super-resolve it to a HR boundary via local self-examples [7]. This technique exploits local scale invariance in natural images upon small scaling factors, which holds for various image singularities such as straight and corner boundaries. The algorithm is simple yet efficient and produces high-quality HR boundaries.

5.2.2. Estimation of the HR Transition Region

We derive the HR borders between the smooth / transition regions from the LR transition region and the super-resolved HR hard boundary. We first compute the *width* of the HR transition region. Assuming a Gaussian filtering degradation process, the correspondence between the width of the LR transition region d_l and that of the HR transition region d_h takes the form

$$d_h = M d_l - \delta_d(M), \tag{3}$$

where $\delta_d(M)$ is a function of M describing the degradation of the low-pass filtering. For example, $\delta_d(M) = 2$ when $M = 2$ with a Gaussian filter of size 3×3. This ensures that the width of the HR transition region is not simply M times the width of the LR transition region, which otherwise will result in a blurred image.

We then derive the HR borders between the smooth / transition regions from the width of the HR transition region computed from (3) and the HR hard boundary. Further, we estimate weights in the HR transition region via polynomial fitting from weights in the corresponding LR transition region. In particular, assuming edge weights perpendicular to the orientation of the HR hard boundary follow the same varying trend in LR / HR transition regions, we first fit edge weights in the LR transition region to a second-order polynomial, and then compute weights in the HR transition region by polynomial fitting within the borders of the HR transition region.

5.3. Problem Formulation

Having constructed the HR graph, we compute its corresponding graph Laplacian matrix $\mathcal{L}_h$ and define the smoothness prior of the

latent HR image patch $\mathbf{z} \in \mathbb{R}^{M^2 N}$ as

$$P(\mathbf{z}) = \mathbf{z}^T \mathcal{L}_h \mathbf{z}, \tag{4}$$

which describes the total variation of $\mathbf{z}$ with respect to the HR graph as discussed in Sec. 3.

Further, in order to measure the reconstruction error, we assume the HR image patch is the Gaussian-low-pass-filtered and down-sampled version of the LR patch. The joint denoising / SR problem is then modelled as

$$\mathbf{y} = DH\mathbf{z} + \mathbf{e}, \tag{5}$$

where $\mathbf{y} \in \mathbb{R}^N$ is the noise-corrupted and LR observation vector, H is a Gaussian low-pass filtering operator, D is a down-sampling matrix, and $\mathbf{e}$ is independent and identically distributed (iid) additive white Gaussian noise (AWGN)[2].

We then formulate the joint denoising / SR problem as an optimization problem regularized by the smoothness prior, which takes the form

$$\min_{\mathbf{z}} \ \|DH\mathbf{z} - \mathbf{y}\|_2^2 + \lambda \mathbf{z}^T \mathcal{L}_h \mathbf{z} \tag{6}$$

where the first term is the data fidelity term describing the reconstruction error, and the second term is the graph smoothness prior. λ is a weighting parameter for the trade-off between the reconstruction error and signal smoothness. This optimization is an unconstrained quadratic programming problem and can thus be efficiently solved.

6. EXPERIMENTATION

6.1. Experimental Setup

We evaluate our proposed joint denoising / SR scheme using two caption images *English* and *Chinese*, one logo image *HKUST* and one depth map *Teddy*[3] (which is piecewise smooth, a special case of GPWS images). AWGN is added to these images, with the standard deviation σ ranging from 10 to 25. We compare our scheme against two representative separable denoising / SR approaches: one performs denoising via Bilateral Filtering (BF) [16] first and then SR via New Edge-Directed Interpolation (NEDI) [17] (called `BF+NEDI` for short), and the other performs Non-Local Means Denoising (NLM) [18] first and then SR via NEDI (called `NLM+NEDI` for short). The parameter λ in (6) is empirically set to 0.1, and M is assigned 2 for evaluation.

6.2. Experimental Results

We first quantitatively measure the denoising / SR results using the structural similarity (SSIM) index [19] to assess image quality. SSIM of the denoised and super-resolved images for different schemes under various noise levels are listed in Table 1. We see that our scheme outperforms `BF+NEDI` and `NLM+NEDI` at all noise levels, with 0.1917 gain over `BF+NEDI` and 0.0624 gain over `NLM+NEDI` in SSIM on average. Further, we see that the performance of our proposed scheme degrades slower than that of `BF+NEDI` as the noise level increases; *i.e.*, our proposal is more robust to increasing noise levels. This is due to the robust identification of hard boundaries and borders between smooth / transition regions at various noise levels.

Fig. 4 shows the subjective comparison of our scheme with `BF+NEDI`. The denoised and super-resolved HR images by our scheme are all sharper than those produced by `BF+NEDI`. This is due to the robust identification of hard boundaries between smooth / transition regions via spectral clustering, while in `BF+NEDI` image structures are increasingly hard to preserve in the denoising step prior to SR. Further, unlike `BF+NEDI`, there remains very little visible noise in the resulting images produced by our scheme.

[2]Though we assume a simple iid noise model in this paper, our proposed graph-based joint denoising / SR framework can be extended to include more complex noise model. We leave this investigation for future work.

[3]http://vision.middlebury.edu/stereo/data/scenes2003/

Table 1. Performance Comparison in SSIM

		σ			
Image	Method	10	15	20	25
English	BF+NEDI	0.8211	0.7433	0.6720	0.5792
	NLM+NEDI	0.8311	0.7800	0.7726	0.6698
	Proposed	**0.8855**	**0.8641**	**0.8356**	**0.8117**
Chinese	BF+NEDI	0.7121	0.6610	0.5821	0.5253
	NLM+NEDI	0.7674	0.7505	0.6747	0.6525
	Proposed	**0.9069**	**0.8850**	**0.8539**	**0.8280**
HKUST	BF+NEDI	0.9707	0.9456	0.8784	0.7894
	NLM+NEDI	0.9786	0.9572	0.9424	0.9245
	Proposed	**0.9791**	**0.9677**	**0.9507**	**0.9321**
Teddy	BF+NEDI	0.8498	0.6636	0.5582	0.4018
	NLM+NEDI	0.9444	0.9225	0.9066	0.8974
	Proposed	**0.9583**	**0.9339**	**0.9244**	**0.9046**

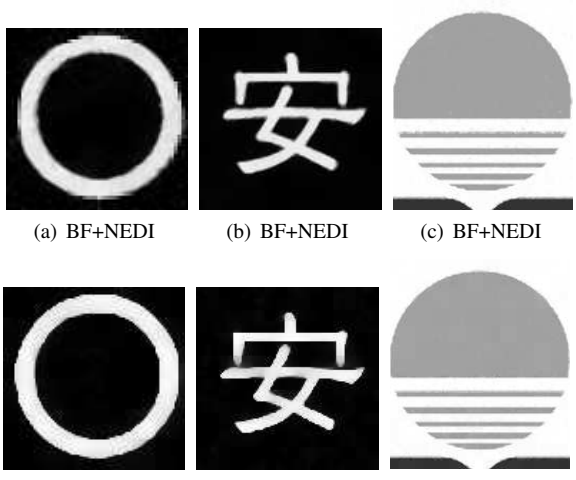

(a) BF+NEDI (b) BF+NEDI (c) BF+NEDI

(d) Proposed (e) Proposed (f) Proposed

Fig. 4. The denoised and super-resolved images of (a)(d) *English* at noise level 20; (b)(e) *Chinese* at noise level 10; and (c)(f) a cropped part of *HKUST* at noise level 10.

7. CONCLUSION

In this paper, we propose to perform joint denoising / SR for GPWS images in one unified graph-theoretic framework. The key observation is that GPWS images imply simple-enough graph representations in the pixel domain, so that suitable graph-based filtering techniques can be readily applied. The graph representation for each GPWS pixel patch is derived via spectral clustering that segments the patch into smooth and transition regions, resulting in the preservation of image structures. Graph weights in the smooth regions are simply assigned 1, and weights in the transition region are robustly computed using an average kernel oriented parallel to the detected hard boundary. Our formulation leads to an unconstrained quadratic programming problem, which can be very efficiently solved. When tested on GPWS images corrupted by AWGN, we show that our algorithm outperforms two representative separable denoising / SR schemes in both subjective and objective quality.

8. REFERENCES

[1] W. Hu, G. Cheung, X. Li, and O. Au, "Depth map compression using multi-resolution graph-based transform for depth-image-based rendering," in *IEEE International Conference on Image Processing*, Orlando, FL, September 2012.

[2] W. Hu, X. Li, G. Cheung, and O. Au, "Depth map denoising using graph-based transform and group sparsity," in *IEEE International Workshop on Multimedia Signal Processing*, Pula, Italy, October 2013.

[3] L. Itti, C. Koch, and E. Niebur, "A model of saliency-based visual attention for rapid scene analysis," in *IEEE Transactions on Pattern Analysis and Machine Intelligence*, November 1998, vol. 20, no.11, pp. 1254–1259.

[4] D. I. Shuman, S. K. Narang, P. Frossard, A. Ortega, and P. Vandergheynst, "The emerging field of signal processing on graphs: Extending high-dimensional data analysis to networks and other irregular domains," in *IEEE Signal Processing Magazine*, May 2013, vol. 30, no.3, pp. 83–98.

[5] P. Milanfar, "A tour of modern image filtering," in *IEEE Signal Processing Magazine*, January 2013, vol. 30, no.1, pp. 106–128.

[6] U. Luxburg, "A tutorial on spectral clustering," in *Statistics and Computing*, December 2007, vol. 17, no.4, pp. 395–416.

[7] Gilad Freedman and Raanan Fattal, "Image and video upscaling from local self-examples," *ACM Trans. Graph.*, vol. 28, no. 3, pp. 1–10, 2010.

[8] K. Hirakawa and T. W. Parks, "Joint demosaicking and denoising," in *IEEE Transactions on Image Processing*, August 2006, vol. 15, no.8, pp. 2146–2157.

[9] L. Zhang, X. Wu, and D. Zhang, "Color reproduction from noisy cfa data of single sensor digital cameras," in *IEEE Transactions on Image Processing*, September 2007, vol. 16, no.9, pp. 2184–2197.

[10] Z. Zheng, B. Wang, and K. Sun, "Single remote sensing image super-resolution and denoising via sparse representation," in *International Workshop on Multi-Platform / Multi-Sensor Remote Sensing and Mapping*, Xiamen, China, January 2011.

[11] L. Zhang, X. Li, and D. Zhang, "Image denoising and zooming under the lmmse framework," in *IET Image Processing*, 2012, vol. 6, no.3, pp. 273–283.

[12] F. K. Chung, "Spectral graph theory," in *American Mathematical Society*, 1997.

[13] A. Sandryhaila and J. Moura, "Discrete signal processing on graphs," in *IEEE Transactions on Signal Processing*, April 2013, vol. 61, NO. 7, pp. 1644–1656.

[14] J. Shi and J. Malik, "Normalized cuts and image segmentation," in *IEEE Transactions on Pattern Analysis and Machine Intelligence*, August 2000, vol. 22, no.8.

[15] H. Takeda, S. Farsiu, and P. Milanfar, "Kernel regression for image processing and reconstruction," in *IEEE Transactions on Image Processing*, February 2007, vol. 16, no.3, pp. 349–366.

[16] C. Tomasi and R. Manduchi, "Bilateral filtering for gray and color images," in *Proceedings of the IEEE International Conference on Computer Vision*, Bombay, India, 1998.

[17] X. Li and M. Ochard, "New edge-directed image interpolation," in *IEEE Transactions Image Processing*, October 2001, vol. 10, no.10, pp. 1521–1527.

[18] A. Buades, B. Coll, and J. Morel, "A non-local algorithm for image denoising," in *IEEE International Conference on Computer Vision and Pattern Recognition (CVPR 2005)*, San Diego, CA, June 2005.

[19] Z. Wang, A. Bovik, H. Sheikh, and E. Simoncelli, "Image quality assessment: From error visibility to structural similarity," in *IEEE Transactions on Image Processing*, August 2005, vol. 13, no.4, pp. 600–612.